

Data report: clay mineral assemblages in cores from Hole C0002P, IODP Expedition 348, Nankai Trough accretionary prism¹

Michael B. Underwood² and Chen Song³

Chapter contents

Abstract	1
Introduction	1
Methods	2
Results	3
Acknowledgments	3
References	3
Figures	7
Tables	11

Abstract

This report summarizes the results of X-ray diffraction analyses of core samples from Integrated Ocean Drilling Program Hole C0002P. Twenty-three specimens were collected from the Nankai accretionary prism over a depth interval of 2163 to 2218 meters below seafloor. Analyses of the <2 mm size fraction show considerable amounts of variation in relative mineral abundances. Percentages of clay-size smectite average 39.5 wt% (standard deviation of 17.9). Percentages of illite and kaolinite + chlorite average 32.4 and 25.1 wt%, respectively (standard deviations of 8.5 and 7.8). Values of illite/smectite expandability average 70%, and the percentage of illite in illite/smectite mixed-layer clays averages 41%. Values of illite crystallinity index are consistent with advanced levels of diagenesis to anchizone metamorphism within detrital source areas.

Introduction

Scientific ocean drilling has targeted the Nankai Trough region, offshore southwest Japan (Fig. F1), several times over the past four decades (Karig, Ingle, et al., 1975; Kagami, Karig, Coulbourn, et al., 1986; Shipboard Scientific Party, 1991; Shipboard Scientific Party, 2001; Moore et al., 2005). The latest drilling efforts are part of the Nankai Trough Seismogenic Zone Experiment (NanTroSEIZE) (Ashi et al., 2009; Sreaton et al., 2009; Tobin et al., 2009; Underwood et al., 2010; Expedition 333 Scientists, 2012). Previous investigators demonstrated that hemipelagic mud(stones) throughout the Nankai region change in composition largely as a function of depositional age (Cook et al., 1975; Chamley, 1980; Chamley et al., 1986; Underwood et al., 1993a, 1993b; Masuda et al., 1996, 2001; Steurer and Underwood, 2003; Underwood and Steurer, 2003; Guo and Underwood, 2012; Underwood and Guo, 2013). As a rule, Miocene strata throughout the region are enriched in smectite, whereas Pliocene and Quaternary deposits contain more detrital illite and chlorite.

Integrated Ocean Drilling Program (IODP) Site C0002 is located near the seaward edge of the Kumano Basin (Fig. F1). IODP Expeditions 338 and 348 used riser drilling at Site C0002 to reach intermediate depths of the accretionary prism (Strasser et al., 2014; see the “Expedition 348 summary” chapter [Tobin et al., 2015a]). The interval that was cored during Expedition 348 ex-

¹Underwood, M.B., and Song, C., 2016. Data report: clay mineral assemblages in cores from Hole C0002P, IODP Expedition 348, Nankai Trough accretionary prism. In Tobin, H., Hirose, T., Saffer, D., Toczko, S., Maeda, L., Kubo, Y., and the Expedition 348 Scientists, *Proceedings of the Integrated Ocean Drilling Program, 348*: College Station, TX (Integrated Ocean Drilling Program). doi:10.2204/iodp.proc.348.202.2016

²Department of Earth and Environmental Science, New Mexico Institute of Mining and Technology, Socorro, New Mexico, USA.

UnderwoodM@missouri.edu

³Department of Geological Sciences, University of Missouri, Columbia, Missouri, USA.



tends from 2163 to 2218 meters below seafloor (mbsf) (Fig. F2). These are the deepest cores ever recovered from an accretionary prism. Beds within that interval dip steeply, generally at angles of 60°–90°. The common lithology is clayey siltstone (hemipelagic mudstone) with thin interbeds of medium silt to fine sand (turbidites) and black bands that were initially thought to contain organic matter. Scanning electron microscopy, coupled with energy dispersive spectroscopy, subsequently showed that the black bands are composed of pyrite (see Song and Underwood, submitted). The cored interval contains nannofossils that are Miocene in age (9.56–10.73 Ma) (see the “Site C0002” chapter [Tobin et al., 2015b]).

One of the broader goals of NanTroSEIZE has been to document the abundances and hydration state of clay minerals (especially the smectite group) within accreted Nankai strata. This is important because of the clay’s likely influence on fluid production within the accretionary prism, as well as along the landward-dipping plate interface (e.g., Saffer et al., 2008). This report summarizes the results of X-ray diffraction (XRD) analyses of 23 core samples extracted from Hole C0002P. We focus on the common clay minerals (smectite, illite, chlorite, and kaolinite) and provide compositional data for whole-round (WR) specimens that other scientists collected for shore-based studies of hydrogeological, frictional, and geotechnical properties.

Methods

Sample preparation

Most of the samples analyzed in this study were selected from co-located “clusters” immediately adjacent to the WR samples used for shipboard analyses of interstitial water chemistry and shore-based tests of frictional, geotechnical, and hydrogeological properties. Each cluster included a specimen for shipboard bulk-powder XRD, which provided estimates of the relative abundance of total clay minerals (see the “Site C0002” chapter [Tobin et al., 2015b]). The extracted WR intervals are shown on Figure F3, as are the XRD sample locations from split cores. We isolated the clay-size fractions for both types by air-drying and gentle hand-crushing of the mudstone with mortar and pestle, after which specimens were immersed in 3% H₂O₂ for at least 24 h to digest organic matter. We added ~250 mL of Na-hexametaphosphate solution (concentration of 4 g/1000 mL distilled H₂O) and inserted the beakers into an ultrasonic bath for several minutes to promote disaggregation and deflocculation. That step (and additional soaking) was repeated until visual inspection

indicated complete disaggregation. Washing consisted of two passes through a centrifuge (8200 revolutions per minute [rpm] for 25 min; ~6000 g) with resuspension in distilled-deionized water after each pass. After transferring the suspended sediment to a 60 mL plastic bottle, each sample was resuspended by vigorous shaking and a 2 min application of a sonic cell probe. The clay-size splits (<2 μm equivalent settling diameter) were then separated by centrifugation (1000 rpm for 2.4 min; ~320 g). Oriented clay aggregates were prepared using the filter-peek method (Moore and Reynolds, 1989) and 0.45 μm membranes. Saturation of the clay aggregates with ethylene glycol vapor occurred in a closed vapor chamber heated to 60°C for at least 24 h prior to XRD analysis.

X-ray diffraction

Our analyses of the core samples from Expedition 348 were completed at the New Mexico Bureau of Geology and Mineral Resources using a Panalytical X’Pert Pro diffractometer with Cu anode. Scans of oriented clay aggregates were run at generator settings of 45 kV and 40 mA. The continuous scans cover an angular range of 3° to 26.5°2θ with a scan step time of 1.6 s and step size of 0.01°2θ. Slits were 1.0 mm (divergence) and 0.1 mm (receiving), and the sample holder was spinning. MacDiff software (version 4.2.5) was used to establish a baseline of intensity, smooth counts, correct peak positions offset by misalignment of the detector (using the quartz [100] peak at 20.95°2θ; d-value = 4.24 Å), and to calculate integrated peak areas (total counts). This program also calculated peak width at half height.

Calculations of mineral abundance

The most accurate analytical methods for XRD analyses require calibration with internal standards, use of single-line reference intensity ratios, and some fairly elaborate sample preparation steps to create optimal random particle orientations (Środoń et al., 2001; Omotoso et al., 2006). Our primary goal throughout the NanTroSEIZE project has been to obtain accurate values for the clay-size fraction from a large suite of samples. To accomplish that goal efficiently, we recorded the integrated areas of a broad smectite (001) peak centered at ~5.3°2θ (d-value = 16.5 Å), the illite (001) peak at ~8.9°2θ (d-value = 9.9 Å), the composite chlorite (002) + kaolinite (001) peak at 12.5°2θ (d-value = 7.06 Å), and the quartz (100) peak at 20.85°2θ (d-value = 4.26 Å). We then applied a matrix of singular value decomposition (SVD) normalization factors (Table T1), which were calculated after analyzing standard mineral mixtures (Underwood et al., 2003). The average errors using

this method were 3.9% for smectite, 1.0% for illite, 1.9% for chlorite, and 1.6% for quartz. The kaolinite (001) and chlorite (002) reflections overlap almost completely, so we followed a refined version of the Biscaye (1964) method, as documented by Guo and Underwood (2011). The average error of accuracy for the chlorite/kaolinite ratio is 2.6%. To calculate the abundance of individual clay minerals in the bulk mudstone, we multiply each relative percentage value among the clay minerals (where smectite + illite + chlorite + kaolinite = 100%) by the percentage of total clay minerals within the bulk powder (where total clay minerals + quartz + feldspar + calcite = 100%), as determined by shipboard XRD analyses of co-located cluster specimens (see the “Site C0002” chapter [Tobin et al., 2015b]). To facilitate direct comparisons with other published data sets from the region, we also report the weighted peak area percentages for smectite, illite, and chlorite + kaolinite using Biscaye (1965) weighting factors (1× smectite, 4× illite, and 2× chlorite + kaolinite). Errors of accuracy using that method can be substantially greater ($\pm 10\%$) than the errors using SVD factors (Underwood et al., 2003).

For documentation of clay diagenesis, we utilized the saddle/peak method of Rettke (1981) to calculate percent expandability of smectite and illite/smectite mixed-layer clay. This method is sensitive to the proportions of discrete illite versus illite/smectite mixed-layer clay; we chose the curve for 1:1 mixtures of discrete illite and illite/smectite. A complementary measure of the proportion of illite in the illite/smectite mixed-layer phase uses the center position ($^{\circ}2\theta$) of the (002/003) peak (following Moore and Reynolds, 1989), using the quartz (100) peak to correct for misalignment of the detector and/or sample holder. We also report illite crystallinity (Kübler) index as values of peak width at half height ($\Delta^{\circ}2\theta$) for the (001) reflection.

Results

Table T2 shows all of the peak-area XRD values (total counts) for common minerals in the clay-size fraction. We also list the calculated values of mineral abundance (wt%) using SVD normalization factors and percentages using the Biscaye (1965) peak-area weighting factors. Relative abundances vary considerably, in accordance with the diverse lithologies recorded in visual core descriptions (Fig. F3). Values for clay-size smectite range from 11.4 to 98.2 wt%, with a mean (μ) of 39.5 wt% and a standard deviation (s) of 17.9. Values for illite range from 1.6 to 46.7 wt% ($\mu = 32.4$; $s = 8.5$). Percentages of kaolinite + chlorite range from 0.1 to 37.0 wt% ($\mu = 25.1$; $s = 7.8$); in all

cases, chlorite is the dominant mineral over kaolinite. Percentages of clay-size quartz range from 0.1 to 13.9 wt% ($\mu = 3.0$; $s = 4.1$). In comparison, mineral abundances in cuttings from the same depth intervals of Hole C0002P are more uniform, and values are close to the averages from core samples (see Underwood, submitted).

Figure F3 shows the exact position of each sample interval on core-scale graphical depictions of lithology. Plotted next to each position are the calculated relative abundances of smectite, illite, and kaolinite + chlorite within the bulk mudstone. Those bulk smectite values range from 4.4 to 71.6 wt% ($\mu = 23.8$; $s = 13.2$). Most percentages of smectite are significantly lower than what Underwood and Guo (2013) documented for coeval Miocene strata (9.56–10.73 Ma) at IODP Sites C0011 and C0012 in the Shikoku Basin (i.e., subduction inputs). Illite in the bulk sediment ranges from 1.2 to 27.6 wt% ($\mu = 18.7$; $s = 4.9$), and kaolinite + chlorite ranges from 0.1 to 21.7 wt% ($\mu = 15.0$; $s = 5.0$).

Indicators of clay diagenesis are tabulated in Table T3. Illite crystallinity (Kübler) indexes range from 0.71 to 0.40 $\Delta^{\circ}2\theta$, with an average value of 0.52 $\Delta^{\circ}2\theta$. As a frame of reference, the upper limit for diagenesis is 0.52 $\Delta^{\circ}2\theta$, and the upper limit for anchizone metamorphism (incipient greenschist facies) is 0.32 $\Delta^{\circ}2\theta$ (Warr and Mählmann, 2015). The expandability of illite/smectite mixed-layer clays ranges from 90% to 62%, with an average value of 70%. The proportion of illite in illite/smectite mixed-layer clays ranges from 13% to 54%, with an average value of 41%.

Acknowledgments

This research used samples provided by the Integrated Ocean Drilling Program (IODP). We thank the Mantle Quest Japan (MQJ) drilling crew, Marine Works Japan (MWJ) laboratory technicians, and fellow scientists aboard the D/V *Chikyu* for their dedicated assistance with sampling during IODP Expedition 348. Funding was granted by the Consortium for Ocean Leadership, U.S. Science Support Program (task order T348B58). Nolan Walla assisted with sample preparation. Rachel Scudder provided a review of the manuscript.

References

- Ashi, J., Lallemand, S., Masago, H., and the Expedition 315 Scientists, 2009. Expedition 315 summary. *In* Kinoshita, M., Tobin, H., Ashi, J., Kimura, G., Lallemand, S., Screaton, E.J., Curewitz, D., Masago, H., Moe, K.T., and the Expedition 314/315/316 Scientists, *Proceedings of the Integrated Ocean Drilling Program*, 314/315/316: Wash-

- ington, DC (Integrated Ocean Drilling Program Management International, Inc.). <http://dx.doi.org/10.2204/iodp.proc.314315316.121.2009>
- Biscaye, P.E., 1964. Distinction between kaolinite and chlorite in recent sediments by X-ray diffraction. *American Mineralogist*, 49:1281–1289. http://www.minso-cam.org/ammin/AM49/AM49_1281.pdf
- Biscaye, P.E., 1965. Mineralogy and sedimentation of recent deep-sea clay in the Atlantic Ocean and adjacent seas and oceans. *Geological Society of America Bulletin*, 76(7):803–831. [http://dx.doi.org/10.1130/0016-7606\(1965\)76\[803:MASORD\]2.0.CO;2](http://dx.doi.org/10.1130/0016-7606(1965)76[803:MASORD]2.0.CO;2)
- Chamley, H., 1980. Clay sedimentation and paleo-environment in the Shikoku Basin since the middle Miocene (Deep Sea Drilling Project Leg 58, North Philippine Sea). In Klein, G. de V., Kobayashi, K., et al., *Initial Reports of the Deep Sea Drilling Project*, 58: Washington, DC (U.S. Govt. Printing Office), 669–678. <http://dx.doi.org/10.2973/dsdp.proc.58.118.1980>
- Chamley, H., Cadet, J.-P., and Charvet, J., 1986. Nankai Trough and Japan Trench late Cenozoic paleo-environments deduced from clay mineralogic data. In Kagami, H., Karig, D.E., Coulbourn, W.T., et al., *Initial Reports of the Deep Sea Drilling Project*, 87: Washington, DC (U.S. Govt. Printing Office), 633–641. <http://dx.doi.org/10.2973/dsdp.proc.87.113.1986>
- Cook, H.E., Zemmels, I., and Matti, J.C., 1975. X-ray mineralogy data, far western Pacific, Leg 31 Deep Sea Drilling Project. In Karig, D.E., Ingle, J.C., Jr., et al., *Initial Reports of the Deep Sea Drilling Project*, 31: Washington (U.S. Govt. Printing Office), 883–895. <http://dx.doi.org/10.2973/dsdp.proc.31.app.1975>
- Expedition 333 Scientists, 2012. Expedition 333 summary. In Henry, P., Kanamatsu, T., Moe, K., and the Expedition 333 Scientists, *Proceedings of the Integrated Ocean Drilling Program*, 333: Tokyo (Integrated Ocean Drilling Program Management International, Inc.). <http://dx.doi.org/10.2204/iodp.proc.333.101.2012>
- Guo, J., and Underwood, M.B., 2011. Data report: refined method for calculating percentages of kaolinite and chlorite from X-ray diffraction data, with application to the Nankai margin of southwest Japan. In Kinoshita, M., Tobin, H., Ashi, J., Kimura, G., Lallemand, S., Screaton, E.J., Curewitz, D., Masago, H., Moe, K.T., and the Expedition 314/315/316 Scientists, *Proceedings of the Integrated Ocean Drilling Program*, 314/315/316: Washington, DC (Integrated Ocean Drilling Program Management International, Inc.). <http://dx.doi.org/10.2204/iodp.proc.314315316.201.2011>
- Guo, J., and Underwood, M.B., 2012. Data report: clay mineral assemblages from the Nankai Trough accretionary prism and the Kumano Basin, IODP Expeditions 315 and 316, NanTroSEIZE Stage 1. In Kinoshita, M., Tobin, H., Ashi, J., Kimura, G., Lallemand, S., Screaton, E.J., Curewitz, D., Masago, H., Moe, K.T., and the Expedition 314/315/316 Scientists, *Proceedings of the Integrated Ocean Drilling Program*, 314/315/316: Washington, DC (Integrated Ocean Drilling Program Management International, Inc.). <http://dx.doi.org/10.2204/iodp.proc.314315316.202.2012>
- Kagami, H., Karig, D.E., Coulbourn, W.T., et al., 1986. *Initial Reports of the Deep Sea Drilling Project*, 87: Washington, DC (U.S. Govt. Printing Office). <http://dx.doi.org/10.2973/dsdp.proc.87.1986>
- Karig, D.E., Ingle, J.C., Jr., et al., 1975. *Initial Reports of the Deep Sea Drilling Project*, 31: Washington, DC (U.S. Govt. Printing Office). <http://dx.doi.org/10.2973/dsdp.proc.31.1975>
- Masuda, H., O'Neil, J.R., Jiang, W.-T., and Peacor, D.R., 1996. Relation between interlayer composition of authigenic smectite, mineral assemblages, I/S reaction rate and fluid composition in silicic ash of the Nankai Trough. *Clays and Clay Minerals*, 44:443–459. <http://dx.doi.org/10.1346/CCMN.1996.0440402>
- Masuda, H., Peacor, D.R., and Dong, H., 2001. Transmission electron microscopy study of conversion of smectite to illite in mudstones of the Nankai Trough: contrast with coeval bentonites. *Clays and Clay Minerals*, 49(2):109–118. <http://dx.doi.org/10.1346/CCMN.2001.0490201>
- Moore, D.M., and Reynolds, R.C., Jr., 1989. Quantitative analysis. In Moore, D.M., and Reynolds, R.C., Jr. (Eds.), *X-Ray Diffraction and the Identification and Analysis of Clay Minerals*: New York (Oxford Univ. Press USA), 272–309.
- Moore, G.F., Mikada, H., Moore, J.C., Becker, K., and Taira, A., 2005. Legs 190 and 196 synthesis: deformation and fluid flow processes in the Nankai Trough accretionary prism. In Mikada, H., Moore, G.F., Taira, A., Becker, K., Moore, J.C., and Klaus, A. (Eds.), *Proceedings of the Ocean Drilling Program, Scientific Results*, 190/196: College Station, TX (Ocean Drilling Program), 1–25. <http://dx.doi.org/10.2973/odp.proc.sr.190196.201.2005>
- Omotoso, O., McCarty, D.K., Hillier, S., and Kleeberg, R., 2006. Some successful approaches to quantitative mineral analysis as revealed by the 3rd Reynolds Cup contest. *Clays and Clay Minerals*, 54(6):748–760. <http://dx.doi.org/10.1346/CCMN.2006.0540609>
- Rettke, R.C., 1981. Probable burial diagenetic and provenance effects on Dakota Group clay mineralogy, Denver Basin. *Journal of Sedimentary Petrology*, 51(2):541–551. <http://dx.doi.org/10.1306/212F7CCF-2B24-11D7-8648000102C1865D>
- Saffer, D.M., Underwood, M.B., and McKiernan, A.W., 2008. Evaluation of factors controlling smectite transformation and fluid production in subduction zones: application to the Nankai Trough. *Island Arc*, 17(2):208–230. <http://dx.doi.org/10.1111/j.1440-1738.2008.00614.x>
- Screaton, E.J., Kimura, G., Curewitz, D., and the Expedition 316 Scientists, 2009. Expedition 316 summary. In Kinoshita, M., Tobin, H., Ashi, J., Kimura, G., Lallemand, S., Screaton, E.J., Curewitz, D., Masago, H., Moe, K.T., and the Expedition 314/315/316 Scientists, *Proceedings of the Integrated Ocean Drilling Program*, 314/315/316: Washington, DC (Integrated Ocean Drilling Program Management International, Inc.). <http://dx.doi.org/10.2204/iodp.proc.314315316.131.2009>
- Shipboard Scientific Party, 1991. Site 808. In Taira, A., Hill, I., Firth, J.V., et al., *Proceedings of the Ocean Drilling Pro-*

- gram, *Initial Reports*, 131: College Station, TX (Ocean Drilling Program), 71–269. <http://dx.doi.org/10.2973/odp.proc.ir.131.106.1991>
- Shipboard Scientific Party, 2001. Leg 190 summary. In Moore, G.F., Taira, A., Klaus, A., et al., *Proceedings of the Ocean Drilling Program, Initial Reports*, 190: College Station, TX (Ocean Drilling Program), 1–87. <http://dx.doi.org/10.2973/odp.proc.ir.190.101.2001>
- Song, C., and Underwood, M.B., submitted. Data report: permeability and microfabric of core samples from IODP Expedition 348, Hole C0002P, Nankai Trough accretionary prism. In Tobin, H., Hirose, T., Saffer, D., Toczko, S., Maeda, L., Kubo, Y., and the Expedition 348 Scientists, *Proceedings of the Integrated Ocean Drilling Program*, 348: College Station, TX (Integrated Ocean Drilling Program).
- Środoń, J., Drits, V.A., McCarty, D.K., Hsieh, J.C.C., and Eberl, D.D., 2001. Quantitative X-ray diffraction analysis of clay-bearing rocks from random preparations. *Clays and Clay Minerals*, 49(6):514–528. <http://ccm.geoscienceworld.org/cgi/content/abstract/49/6/514>
- Steurer, J.F., and Underwood, M.B., 2003. Clay mineralogy of mudstones from the Nankai Trough reference Sites 1173 and 1177 and frontal accretionary prism Site 1174. In Mikada, H., Moore, G.F., Taira, A., Becker, K., Moore, J.C., and Klaus, A. (Eds.), *Proceedings of the Ocean Drilling Program, Scientific Results*, 190/196: College Station, TX (Ocean Drilling Program), 1–37. <http://dx.doi.org/10.2973/odp.proc.sr.190196.211.2003>
- Strasser, M., Dugan, B., Kanagawa, K., Moore, G.F., Toczko, S., Maeda, L., Kido, Y., Moe, K.T., Sanada, Y., Esteban, L., Fabbri, O., Geersen, J., Hammerschmidt, S., Hayashi, H., Heirman, K., Hüpers, A., Jurado Rodriguez, M.J., Kameo, K., Kanamatsu, T., Kitajima, H., Masuda, H., Milliken, K., Mishra, R., Motoyama, I., Olcott, K., Oohashi, K., Pickering, K.T., Ramirez, S.G., Rashid, H., Sawyer, D., Schleicher, A., Shan, Y., Skarbek, R., Song, I., Takeshita, T., Toki, T., Tudge, J., Webb, S., Wilson, D.J., Wu, H.-Y., and Yamaguchi, A., 2014. Expedition 338 summary. In Strasser, M., Dugan, B., Kanagawa, K., Moore, G.F., Toczko, S., Maeda, L., and the Expedition 338 Scientists, *Proceedings of the Integrated Ocean Drilling Program*, 338: Yokohama (Integrated Ocean Drilling Program). <http://dx.doi.org/10.2204/iodp.proc.338.101.2014>
- Tobin, H., Hirose, T., Saffer, D., Toczko, S., Maeda, L., Kubo, Y., Boston, B., Broderick, A., Brown, K., Crespo-Blanc, A., Even, E., Fuchida, S., Fukuchi, R., Hammerschmidt, S., Henry, P., Josh, M., Jurado, M.J., Kitajima, H., Kitamura, M., Maia, A., Otsubo, M., Sample, J., Schleicher, A., Sone, H., Song, C., Valdez, R., Yamamoto, Y., Yang, K., Sanada, Y., Kido, Y., and Hamada, Y., 2015a. Expedition 348 summary. In Tobin, H., Hirose, T., Saffer, D., Toczko, S., Maeda, L., Kubo, Y., and the Expedition 348 Scientists, *Proceedings of the Integrated Ocean Drilling Program*, 348: College Station, TX (Integrated Ocean Drilling Program). <http://dx.doi.org/10.2204/iodp.proc.348.101.2015>
- Tobin, H., Hirose, T., Saffer, D., Toczko, S., Maeda, L., Kubo, Y., Boston, B., Broderick, A., Brown, K., Crespo-Blanc, A., Even, E., Fuchida, S., Fukuchi, R., Hammerschmidt, S., Henry, P., Josh, M., Jurado, M.J., Kitajima, H., Kitamura, M., Maia, A., Otsubo, M., Sample, J., Schleicher, A., Sone, H., Song, C., Valdez, R., Yamamoto, Y., Yang, K., Sanada, Y., Kido, Y., and Hamada, Y., 2015b. Site C0002. In Tobin, H., Hirose, T., Saffer, D., Toczko, S., Maeda, L., Kubo, Y., and the Expedition 348 Scientists, *Proceedings of the Integrated Ocean Drilling Program*, 348: College Station, TX (Integrated Ocean Drilling Program). <http://dx.doi.org/10.2204/iodp.proc.348.103.2015>
- Tobin, H., Kinoshita, M., Ashi, J., Lallemand, S., Kimura, G., Screaton, E.J., Moe, K.T., Masago, H., Curewitz, D., and the Expedition 314/315/316 Scientists, 2009. NanTroSEIZE Stage 1 expeditions: introduction and synthesis of key results. In Kinoshita, M., Tobin, H., Ashi, J., Kimura, G., Lallemand, S., Screaton, E.J., Curewitz, D., Masago, H., Moe, K.T., and the Expedition 314/315/316 Scientists, *Proceedings of the Integrated Ocean Drilling Program*, 314/315/316: Washington, DC (Integrated Ocean Drilling Program Management International, Inc.). <http://dx.doi.org/10.2204/iodp.proc.314315316.101.2009>
- Underwood, M.B., submitted. Data report: clay mineral assemblages and illite/smectite diagenesis in cuttings from Hole C0002P, IODP Expedition 348, Nankai Trough accretionary prism. In Tobin, H., Hirose, T., Saffer, D., Toczko, S., Maeda, L., Kubo, Y., and the Expedition 348 Scientists, *Proceedings of the Integrated Ocean Drilling Program*, 348: College Station, TX (Integrated Ocean Drilling Program).
- Underwood, M.B., Basu, N., Steurer, J., and Udas, S., 2003. Data report: normalization factors for semiquantitative X-ray diffraction analysis, with application to DSDP Site 297, Shikoku Basin. In Mikada, H., Moore, G.F., Taira, A., Becker, K., Moore, J.C., and Klaus, A. (Eds.), *Proceedings of the Ocean Drilling Program, Scientific Results*, 190/196: College Station, TX (Ocean Drilling Program), 1–28. <http://dx.doi.org/10.2973/odp.proc.sr.190196.203.2003>
- Underwood, M.B., and Guo, J., 2013. Data report: clay mineral assemblages in the Shikoku Basin, NanTroSEIZE subduction inputs, IODP Sites C0011 and C0012. In Saito, S., Underwood, M.B., Kubo, Y., and the Expedition 322 Scientists, *Proceedings of the Integrated Ocean Drilling Program*, 322: Tokyo (Integrated Ocean Drilling Program Management International, Inc.). <http://dx.doi.org/10.2204/iodp.proc.322.202.2013>
- Underwood, M.B., Orr, R., Pickering, K., and Taira, A., 1993a. Provenance and dispersal patterns of sediments in the turbidite wedge of Nankai Trough. In Hill, I.A., Taira, A., Firth, J.V., et al., *Proceedings of the Ocean Drilling Program, Scientific Results*, 131: College Station, TX (Ocean Drilling Program), 15–34. <http://dx.doi.org/10.2973/odp.proc.sr.131.105.1993>
- Underwood, M.B., Pickering, K., Gieskes, J.M., Kastner, M., and Orr, R., 1993b. Sediment geochemistry, clay mineralogy, and diagenesis: a synthesis of data from Leg 131, Nankai Trough. In Hill, I.A., Taira, A., Firth, J.V., et al., *Proceedings of the Ocean Drilling Program, Scientific*

- Results*, 131: College Station, TX (Ocean Drilling Program), 343–363. <http://dx.doi.org/10.2973/odp.proc.sr.131.137.1993>
- Underwood, M.B., Saito, S., Kubo, Y., and the Expedition 322 Scientists, 2010. Expedition 322 summary. In Saito, S., Underwood, M.B., Kubo, Y., and the Expedition 322 Scientists, *Proceedings of the Integrated Ocean Drilling Program*, 322: Tokyo (Integrated Ocean Drilling Program Management International, Inc.). <http://dx.doi.org/10.2204/iodp.proc.322.101.2010>
- Underwood, M.B., and Steurer, J.F., 2003. Composition and sources of clay from the trench slope and shallow accretionary prism of Nankai Trough. In Mikada, H., Moore, G.F., Taira, A., Becker, K., Moore, J.C., and Klaus, A. (Eds.), *Proceedings of the Ocean Drilling Program, Scientific Results*, 190/196: College Station, TX (Ocean Drilling Program), 1–28. <http://dx.doi.org/10.2973/odp.proc.sr.190196.206.2003>
- Warr, L.N., and Mählmann, R.F., 2015. Recommendations for Kübler Index standardization. *Clay Minerals*, 50(3):283–286. <http://dx.doi.org/10.1180/clay-min.2015.050.3.02>
- Initial receipt:** 1 March 2016
Acceptance: 26 July 2016
Publication: 30 November 2016
MS 348-202

Figure F1. Map of the Nankai Trough and Kumano Basin study area (NanTroSEIZE transect) with locations of Sites C0002, C0011, and C0012.

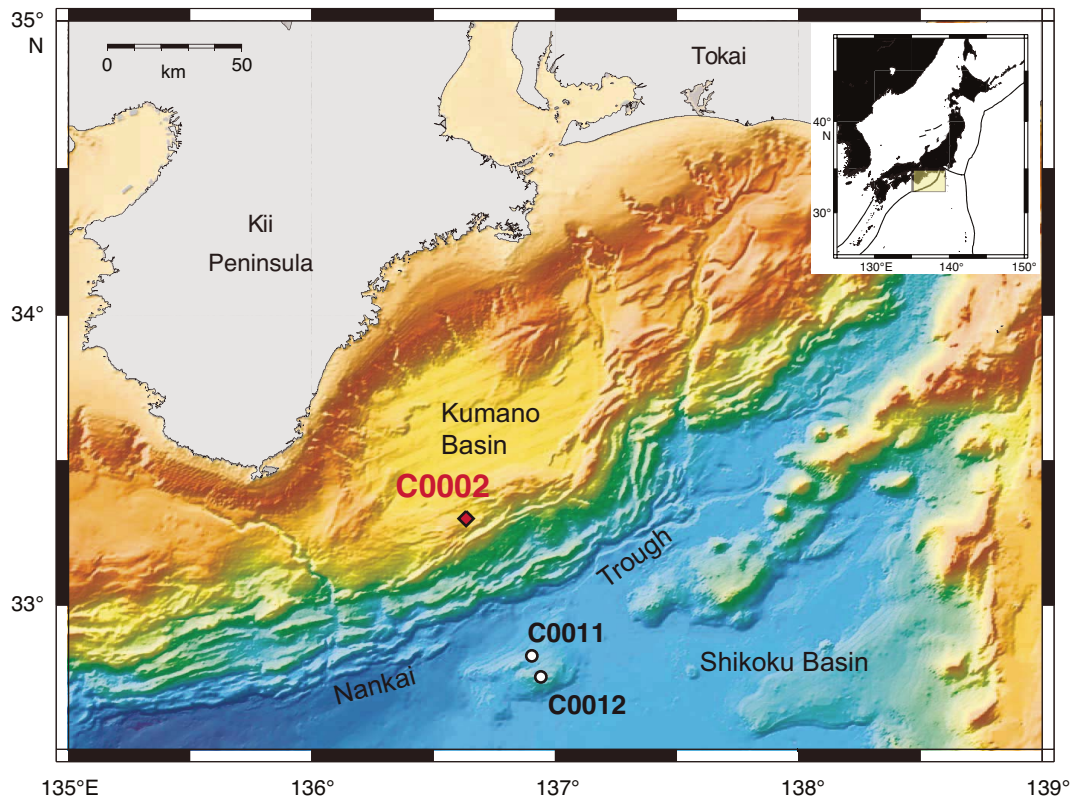


Figure F2. Seismic in-line section crossing Kumano Basin showing location of Site C0002 and lithologic units defined by shipboard analyses of logs, cores, and cuttings (see the “Expedition 348 summary” chapter [Tobin et al., 2015a]). LWD = logging while drilling. VE = vertical exaggeration.

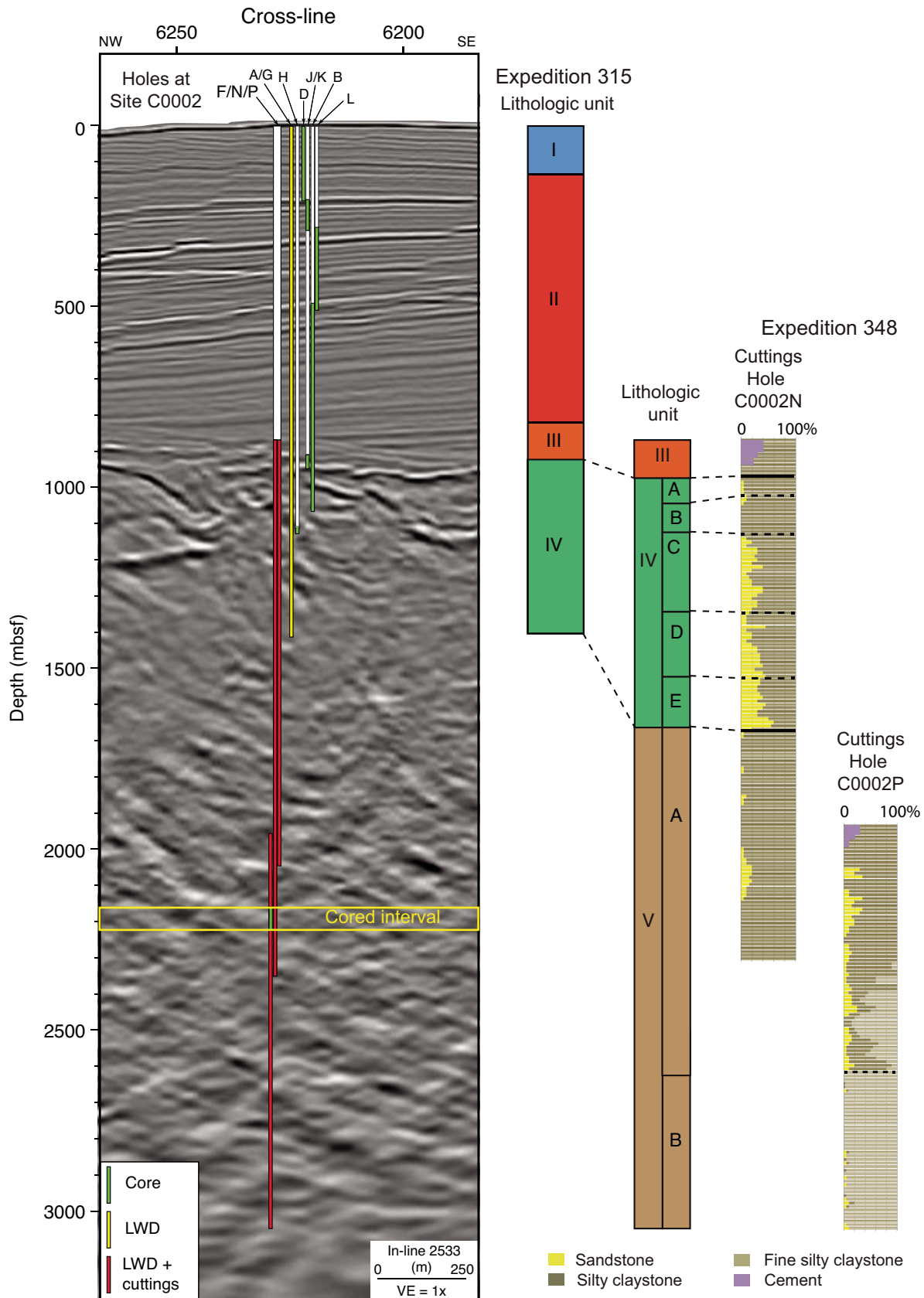


Figure F3. Graphical depictions of cores from Hole C0002P with locations of samples analyzed by X-ray diffraction (red dots) and intervals extracted for whole-round specimens. Modified from visual core descriptions (see the “Site C0002” chapter [Tobin et al., 2015b]). Dominant lithologies include fine sandstone (yellow) and silty claystone (olive gray). Also shown are calculated weight percentages of smectite (S), illite (I), and kaolinite + chlorite (K/C) within the bulk sediment. (Continued on next page.)

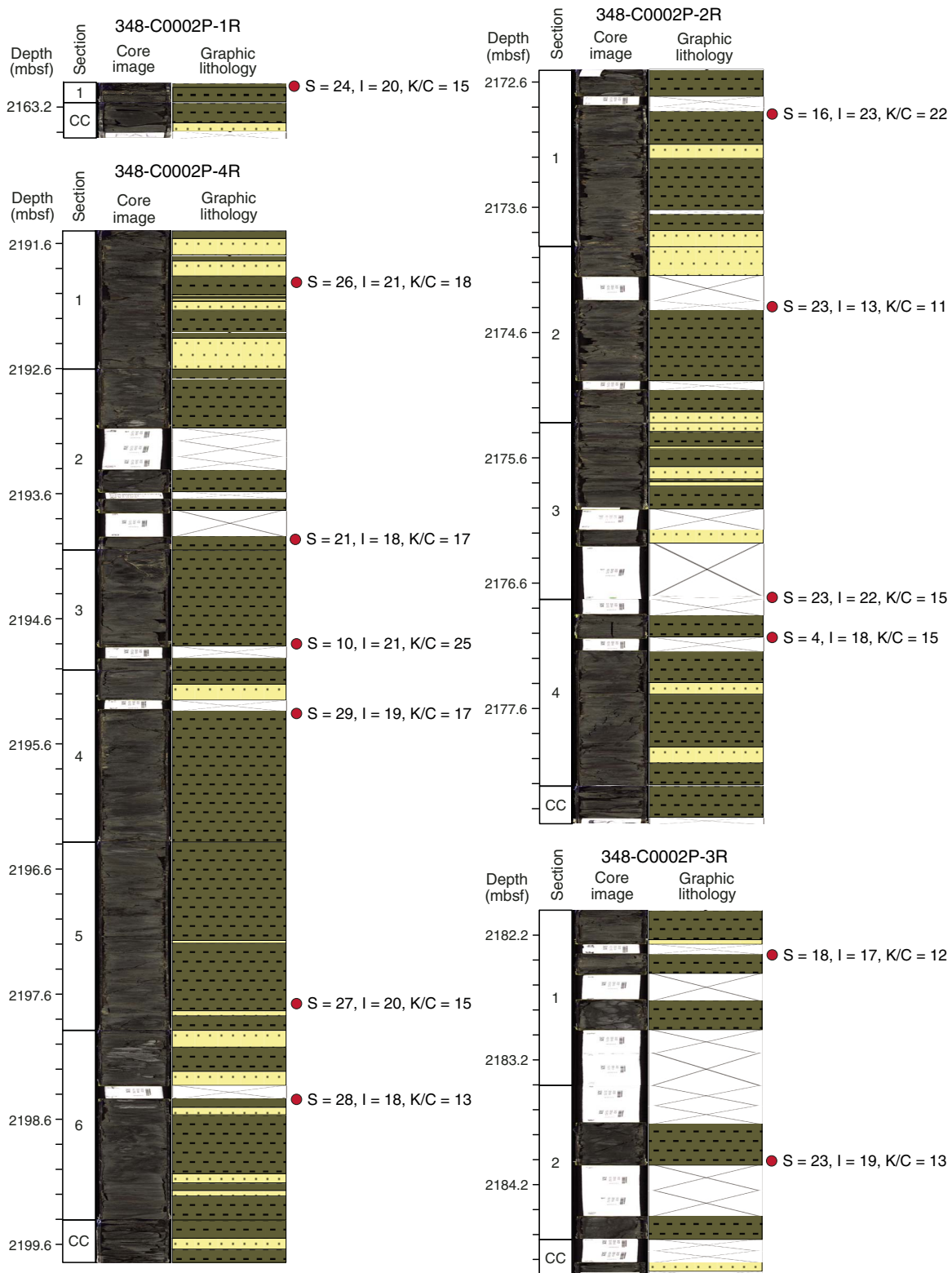


Figure F3 (continued). tr = trace.

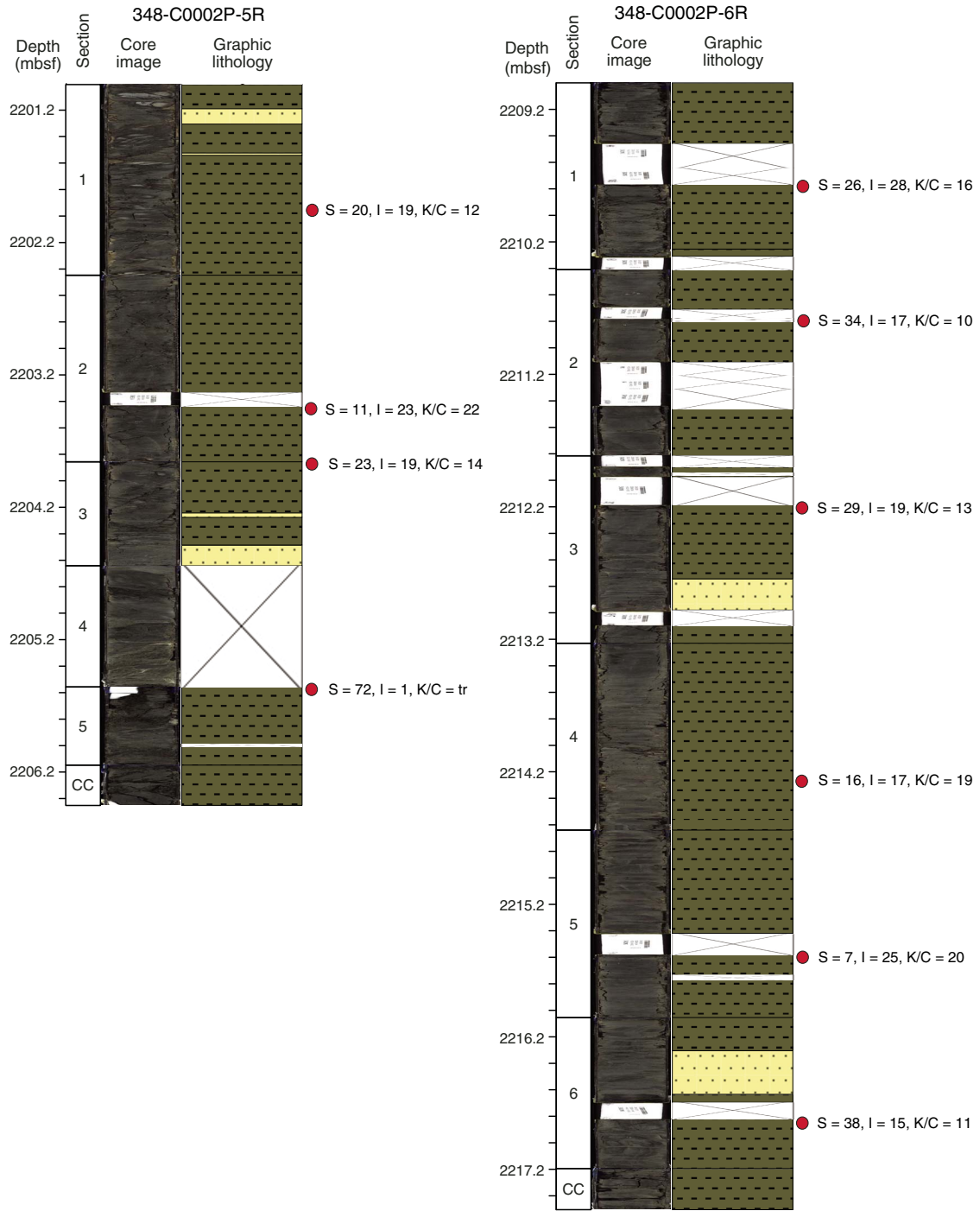


Table T1. Matrix of normalization factors used to calculate relative mineral abundances in clay-size aggregates, derived from singular value decomposition of data from standards.

Influencing mineral	Target mineral in standard mixture			
	Smectite	Illite	Chlorite	Quartz
Smectite	7.4475294E-04	-3.1953641E-05	-7.5067212E-05	-1.5661915E-04
Illite	6.3114654E-05	3.7866938E-03	8.4222964E-05	1.1769286E-04
Chlorite	-3.5636057E-04	-6.7378140E-05	2.5121504E-03	5.2290707E-05
Quartz	9.3573136E-03	3.6491468E-03	3.2755411E-03	1.4825645E-02



Table T2. Results of X-ray diffraction analyses (<2 µm size fraction) for core samples, Hole C0002P.

Core, section, interval (cm)	Depth (mbsf)	Integrated peak area (total counts)				Relative abundance in clay-size fraction								Relative abundance bulk sediment (wt%)				
		Smectite (001)	Illite (001)	Kaolinite (001) + chlorite (002)	Quartz (100)	SVD normalization factors (wt%)				Biscaye factors (%)				Total clay minerals	Smectite	Illite	Kaolinite + chlorite	
		Smectite	Illite	Kaolinite + chlorite	Quartz	Smectite	Illite	Kaolinite + chlorite	Quartz	Kaolinite	Chlorite	Smectite	Illite	Kaolinite + chlorite		Smectite	Illite	Kaolinite + chlorite
348-C0002P-																		
1R-1, 0	2,163.00	22,516	4,061	4,370	384	39.2	32.4	22.4	5.9	6.9	15.5	47	34	18	61.2	24.0	19.9	14.6
2R-1, 35	2,172.85	26,787	7,192	10,257	259	26.6	37.0	35.0	1.4	0.0	35.0	35	38	27	61.1	16.3	22.6	21.7
2R-2, 43	2,174.35	33,527	4,156	5,538	337	47.8	28.1	23.2	0.9	0.0	23.2	55	27	18	47.8	22.8	13.4	11.2
2R-3, 137	2,176.70	30,294	5,928	6,196	160	38.1	37.1	24.6	0.2	6.4	18.2	46	36	19	59.6	22.7	22.1	14.7
2R-4, 27	2,177.00	7,071	5,318	6,123	160	11.4	46.7	36.8	5.1	0.0	36.8	17	52	30	38.5	4.4	18.0	14.9
3R-1, 35	2,182.35	31,520	6,164	6,868	200	37.5	36.4	25.9	0.2	4.8	21.0	45	35	20	47.1	17.7	17.2	12.2
3R-2, 60	2,184.01	29,477	5,168	5,367	338	41.2	34.1	22.4	2.2	1.6	20.8	48	34	18	56.1	23.1	19.1	12.9
4R-1, 39	2,191.89	24,111	4,130	5,327	304	39.0	31.7	26.3	3.0	1.4	24.9	47	32	21	67.4	26.3	21.4	18.3
4R-2, 135	2,193.96	24,563	4,478	6,115	267	36.8	32.6	28.8	1.9	2.5	26.3	45	33	22	56.6	20.8	18.4	16.6
4R-3, 72	2,194.77	5,913	2,768	4,418	264	17.3	34.5	37.0	11.2	11.0	26.1	23	43	34	60.5	10.4	20.9	25.2
4R-4, 32	2,195.33	38,215	5,278	7,458	364	44.1	29.2	26.1	0.6	0.0	26.1	52	28	20	66.3	29.2	19.4	17.4
4R-5, 125	2,197.64	38,676	5,936	6,967	362	43.7	32.1	23.7	0.5	0.0	23.7	51	31	18	62.5	27.3	20.1	14.9
4R-6, 54	2,198.43	37,668	5,081	6,068	311	47.1	30.3	22.4	0.2	0.2	22.2	54	29	17	59.9	28.2	18.2	13.4
5R-1, 95	2,201.95	28,303	5,381	5,595	275	39.3	35.9	23.7	1.0	8.3	15.5	46	35	18	51.7	20.3	18.6	12.4
5R-2, 99	2,203.43	3,225	1,940	2,316	206	17.5	37.7	30.9	13.9	5.1	25.8	21	50	30	60.3	10.5	22.7	21.6
5R-3, 0	2,203.85	29,114	5,091	5,735	288	40.5	34.0	24.3	1.1	0.5	23.9	48	33	19	56.1	22.7	19.1	13.8
5R-5, 2	2,205.57	128,967	1,143	1,018	403	98.2	1.6	0.1	0.1	0.0	0.1	95	3	2	72.9	71.6	1.2	0.1
6R-1, 77	2,209.77	27,740	6,108	5,615	275	36.8	39.0	22.9	1.3	0.0	22.9	44	39	18	70.7	26.1	27.6	16.4
6R-2, 37	2,210.78	48,928	5,147	5,456	411	55.5	27.4	17.0	0.1	0.0	17.0	61	26	14	60.9	33.8	16.7	10.3
6R-3, 37	2,212.19	42,322	5,749	6,426	322	47.7	30.9	21.2	0.1	4.5	16.7	54	29	16	59.8	28.5	18.5	12.7
6R-4, 103	2,214.26	17,269	3,669	6,126	323	30.1	30.4	33.4	6.1	1.7	31.6	39	33	28	54.4	16.4	16.6	19.3
6R-5, 94	2,215.58	4,531	4,004	4,159	277	13.2	43.8	31.6	11.4	0.0	31.6	16	56	29	56.0	7.4	24.5	20.0
6R-6, 77	2,216.83	52,858	4,368	5,823	311	59.3	22.9	17.7	0.1	1.4	16.3	65	21	14	63.8	37.9	14.6	11.3
					Mean:	39.5	32.4	25.1	3.0	2.4	22.7	46	34	20	58.7	23.8	18.7	15.0
					Standard deviation:	17.9	8.5	7.8	4.1	3.2	7.7	16.9	10.6	6.9	7.7	13.2	4.9	5.0

Biscaye (1965) weighting factors: 1× smectite, 4× illite, 2× chlorite + kaolinite. SVD = singular value decomposition.

Table T3. Illite/smectite expandability values, illite abundance in illite/smectite (I/S) mixed-layer clay, and illite crystallinity index for core samples (<2 μm size fraction), Hole C0002P.

Core, section, interval (cm)	Depth (mbsf)	Intensity saddle (cps)	Intensity peak (cps)	Ratio saddle: peak	Expandability (%)	I (002) + S (003) ($^{\circ}2\theta$)	Illite in I/S (%)	Illite crystallinity ($\Delta^{\circ}2\theta$)
348-C0002P-								
1R-1, 0	2163.00	195	308	0.63	65	16.15	42	0.52
2R-1, 35	2172.85	276	393	0.70	62	16.37	53	0.50
2R-2, 43	2174.35	233	439	0.53	69	16.06	34	0.45
2R-3, 137	2176.70	236	416	0.57	68	16.21	46	0.52
2R-4, 27	2177.00	160	192	0.83	65	16.42	54	0.47
3R-1, 35	2182.35	247	433	0.57	68	15.92	23	0.53
3R-2, 60	2184.01	227	390	0.58	67	16.20	45	0.50
4R-1, 39	2191.89	154	297	0.52	70	16.26	48	0.53
4R-2, 135	2193.96	210	322	0.65	64	16.42	54	0.50
4R-3, 72	2194.77		Peak not properly resolved			16.27	49	0.71
4R-4, 32	2195.33	250	456	0.55	69	15.98	27	0.52
4R-5, 125	2197.64	264	484	0.55	69	16.18	44	0.46
4R-6, 54	2198.43	232	457	0.51	71	16.25	48	0.58
5R-1, 95	2201.95	208	375	0.55	68	16.27	49	0.56
5R-2, 99	2203.43		Peak not properly resolved			16.07	35	0.62
5R-3, 0	2203.85	222	365	0.61	66	16.23	47	0.47
5R-5, 2	2205.57	201	1387	0.14	90	15.82	13	0.40
6R-1, 77	2209.77	260	392	0.66	64	16.37	53	0.51
6R-2, 37	2210.78	194	514	0.38	78	16.04	31	0.52
6R-3, 37	2212.19	248	489	0.51	71	16.10	39	0.51
6R-4, 103	2214.26	66	172	0.38	77	16.16	43	0.54
6R-5, 94	2215.58		Peak not properly resolved			16.21	46	0.69
6R-6, 77	2216.83	224	609	0.37	78	16.03	30	0.45
				Mean:	69.9		41.3	0.52
				Standard deviation:	6.5		10.9	0.07

cps = counts per step.